Experimental Electron-Transfer Cross Sections for Fluorine Ions in Argon at Energies from 8 to 54 MeV*

S. M. Ferguson,† J. R. Macdonald, T. Chiao, L. D. Ellsworth, and S. A. Savoy
Department of Physics, Kansas State University, Manhattan, Kansas 66506
(Received 12 March 1973)

Electron-capture and -loss cross sections have been measured for fluorine ions passing through argon gas in the energy range from 8 to 54 MeV. Cross sections for single- and multiple-electron capture and loss in a single collision were obtained using a computer analysis in real time for fitting the data with an iterative procedure. A detailed description of the computer analysis is given. The capture of as many as four electrons in a single collision has been observed in several cases. The velocity dependence of the single-capture cross section is described by a power of velocity with the power generally increasing for lower-incident-charge states. For multiple-capture processes the cross section decreases more rapidly than a power of velocity. The capture cross section for the fully stripped fluorine nucleus amounts to less than 50% of the theoretical predictions of Nikolaev scaled from a Brinkman-Kramers calculation for protons in argon. The ratio of double- to single-electron-capture cross sections has been discussed in terms of a geometry-independent component of the capture process. The maxima observed in this ratio were rather sharp and close to the same energy for all incident-charge states, making it impossible to identify from the excitation functions the specific shells involved in the capture process. Electron-loss cross sections generally exhibit a broad maximum at velocities approximately twice the orbital velocity of the electron that is lost in the collision. The velocity dependence of multiple-loss cross sections is generally not similar to those for single loss.

I. INTRODUCTION

A program of experimental investigations of the interaction of fast charged particles with matter is under way at the Kansas State University tandem-accelerator laboratory. One of the first results of that program is our recently published paper on the electron-transfer cross sections for fluorine ions in nitrogen.[1] In Ref. 1 we reviewed briefly the experimental and theoretical investigation by other workers of charge exchange by ions with $Z \lesssim 10$. In addition, a comprehensive review of the field with particular emphasis on ions with $Z \gtrsim 16$ has recently been published by Betz.[2] In this paper, charge-exchange cross sections for fluorine ions in collision with argon atoms are reported, and the details are given of the computer analysis used to extract single- and multiple-transfer cross sections from the charge-fraction distributions that are measured as a function of target thickness.

Because this computer analysis is done in real time concurrent with the acquisition of the experimental data, the approximations and iterative procedures that are used to obtain cross sections rapidly and reliably are given.

II. EXPERIMENTAL

Fluorine ions in the energy range from 8 to 54 MeV [corresponding to velocities from (0.9 to 2.4) $\times 10^9$ cm/s] were provided by the EN Tandem Van de Graaff accelerator of Kansas State University. The beam-handling equipment and the differentially pumped target-gas cell were described in Ref. 1. Ions emerging from the gas cell were deflected in a magnetic field and detected in a 5-cm-long position-sensitive detector provided by Nuclear Diodes, Inc. This detector permitted greater separation of the peaks of adjacent charge states, so that better position resolution was provided than with the 2-cm detector used in Ref. 1. Hence the charge fractions were determined by direct pulse-height analysis of the position-energy product signal without removing the energy dependence by analog division.

At each selected energy of the fluorine ions, and with all incident-charge states from +4 to +9, charge spectra were taken with five or more different gas pressures from 0.1 to 10 μ in the gas cell. More than 10^5 ions were counted in each spectrum, permitting a statistical accuracy of 3% for charge fractions equal to 0.01 and 10% for charge fractions equal to 0.001. The charge states were well separated in the detector, and in summing the peaks in the position spectra counts originating from adjacent charge states were negligible. Background in the spectra originated from both slit-edge scattering and charge exchange in the residual gas in front of the target chamber. Both these contributions were independent of pressure in the gas cell and were 0.5% or less of the

incident beam under conditions with no gas in the cell. Thin-target conditions were met in this experiment, using the criterion that the incident-charge fraction be maintained greater than 92% for all pressures used in the calculation of cross sections. A comparison of cross sections determined at different times indicates that the pressure can be maintained in the gas cell with a reproducibility of about 1%. The absolute pressure calibration of the capacitance manometer is better than 10%.

A major source of systematic error in measurements of this kind results from the difficulty in attaining gas cell, magnet, and detector alignment that ensures the same efficiency of detection and background for all charge states in the 5-mm-wide detector. Because peak intensities differing by more than 10^3 are determined concurrently, the error from overlap of tails of large peaks with charge fractions $\lesssim 0.005$ has been observed to change by up to 30%, with as small as 1° misalignment of the detector axis to the plane on which the charge states are spatially separated by the magnetic field. The magnitude of this effect is dependent on the beam-handling conditions, the amount of slit-edge scatter, and the acceptance angle of the detector for particles scattered from the gas target. For these experiments beam collimation of ~0.1° was provided by the 1-mm entrance aperture to the cell and a 3-mm slit system about 4 m in front of the gas cell. This arrangement provided minimum slit-edge scatter and gave a geometric spot size ~2 mm in diameter on the detector. However, with gas in the cell the beam spots broaden slightly from scattering in the target. The exit apertures of the gas cell permitted all particles scattered by less than 3° to emerge, although only those scattered by less than 0.3° perpendicular to the plane of the deflection magnet were observed in the detector. If the system is perfectly aligned no error results from ignoring particles scattered by >0.3°, but because of the deflection up to 5 cm in the plane of the magnet, large errors can be generated if there is a small misalignment of the detector axis and magnet plane. This error was minimized by comparing data taken at several different magnetic field settings and detector positions. The scatter in the cross sections which are presented in Figs. 2 and 5 reflects the extent to which the results are influenced by this systematic error.

III. DATA ANALYSIS

The equations which describe the fraction of ions $\phi_i(x)$ in a given charge state i after passing through a material of thickness x are

$$\frac{d\phi_i(x)}{dx} = \sum_{j \neq 1} (\sigma_{j\,i}\,\phi_j - \sigma_{i\,j}\,\phi_i), \tag{1}$$

where $\sigma_{j\,i}$ is the cross section for the transition from charge state j to i. The cross section so defined will depend upon the excitation state of the incident beam and the density of the target gas. The flight time to the gas target after the equilibrating foil ranges from 30 to 100 μs, and the cross sections reported in this paper for each charge state are representative of mixtures of any metastable states of comparable lifetimes, as well as states produced by excitation in the thin-gas target. The measured cross sections are for single-charge-exchange collisions in a gas with a pressure of from 1 to 10 μ.

In order to extract the set of charge-exchange cross sections at a given energy, one can measure a set of charge fractions ϕ_i for several values of x and solve Eq. (1) for $\sigma_{i\,j}$. In principle this can be done using measurements of $\phi_i(x)$ over any region of x for which the charge fractions have not reached equilibrium values. Details of a least-squares technique to extract cross sections have been published by Datz *et al.*[3] However, in practice it is difficult to extract multiple-transfer cross sections in the presence of large single-transfer cross sections, even under thin-target conditions, unless initial conditions that permit independent determination of the cross sections are selected. Under thin-target conditions first-order estimates of the set of cross sections that connect the experimental incident-charge state with all final states can be made by assuming that each cross section is proportional to the growth of the relevant charge state with target thickness. A complete first-order set of cross sections can then be used to integrate numerically Eq. (1) to calculate charge fractions as a function of target thickness. An iterative procedure can be followed to minimize in a least-squares sense the difference between experimental and calculated charge fractions to an accuracy commensurate with the experimental uncertainty in the data. Although the analysis used in the present work is essentially the same as that described above, it has been specifically designed to permit use of a small on-line computer for which the size of the core available for real-time analysis is restricted while data are accumulating. To accomplish this, we have found it necessary to limit to six the number of different pressures for which charge-fraction sets were measured with each incident charge state.

In addition, to restrict the number of iterations required to fit Eq. (1) it is necessary that the first-order estimates of the cross sections not

only be as accurate as possible but also be changed systematically with each iteration. Rather than use the "slope method"[2,3] for estimating first-order cross sections with uncertainties arising from both pressure variations and counting statistics, we have used the method developed by Macdonald and Martin[4] to obtain relative first-order cross sections from each incident-charge state with uncertainties from statistics of the counts in the relevant peaks of the charge-state spectra only. Clearly, the absolute cross sections have uncertainties from pressure variation as well. It is important to point out that the strength of this technique of analysis depends on being able to measure charge-fraction growth with target thickness for thin-target conditions for *all* initial-charge states. Starting with the first-order cross sections to integrate Eq. (1) we have found that the final cross sections accurate to experimental uncertainties could be obtained almost always in two iterations. The details of the analysis are summarized in the following discussion.

The criterion of thin-target conditions throughout our experiments is that $\phi_\alpha \gg \phi_i \ (i \neq \alpha)$ where α is the incident-charge state. To obtain the first-order estimate of the cross sections this condition implies that $\sigma_{\alpha i}\,\phi_\alpha \gg \sigma_{i\alpha}\phi_i \ (i \neq \alpha)$. This assumption is generally valid for incident-charge states far from the equilibrium mean charge but valid for the incident states near equilibrium only if the incident-charge fraction is kept close to unity. Using this assumption, Eq. (1) can be reduced to

$$\frac{d\phi_\alpha(x)}{dx} = \sum_{j\neq\alpha} -\sigma_{\alpha j}\,\phi_\alpha(x), \qquad \frac{d\phi_i(x)}{dx} = \sigma_{\alpha i}\phi_\alpha(x). \tag{2}$$

Equations (2) yield the approximate solutions

$$\phi_\alpha(x) = \phi_\alpha(0)\, e^{-S_\alpha x}, \qquad \phi_i(x) = \frac{\sigma_{\alpha i}}{S_\alpha}\left[1 - \phi_\alpha(x)\right], \tag{3}$$

where $S_\alpha = \sum_{j\neq\alpha}\sigma_{\alpha j}$ is the total charge-exchange cross section from the state α. The first step in our computer program has been written to extract the first-order total cross section S_α and all relative cross sections $\sigma_{\alpha i}/S_\alpha$ by fitting the experimental data at six pressures for each incident charge with Eqs. (3) using a least-squares procedure. This technique permits small relative cross sections to be obtained to a good approximation independent of all target-thickness uncertainties by using the incident-charge fraction as the independent variable in our fitting procedure. The slope method may not permit this unless data are taken at a somewhat larger number of pressures. These first-order cross sections were calculated while the data were being taken with the next incident-charge state.

After a set of cross sections has been obtained for all incident-charge states that are populated at a particular energy, Eq. (1) can be integrated numerically to obtain charge fractions as a function of target thickness starting with the experimental initial conditions. In Fig. 1 a comparison is presented between experimental data points given by symbols and the charge fractions calculated from first-order cross sections given by the dashed lines. In this example the incident ions were 35-MeV fluorine in the +5 charge state. At the top of Fig. 1 ϕ_5 is plotted logarithmically as a function of target thickness, and at the bottom the other ϕ_i's are plotted as a function of the charge-5 fraction. Fractions calculated to second order are shown by the solid lines.

In our derivation of Eqs. (2) we have assumed, in effect, that the ions make only one charge-changing collision. The limited validity of this assumption

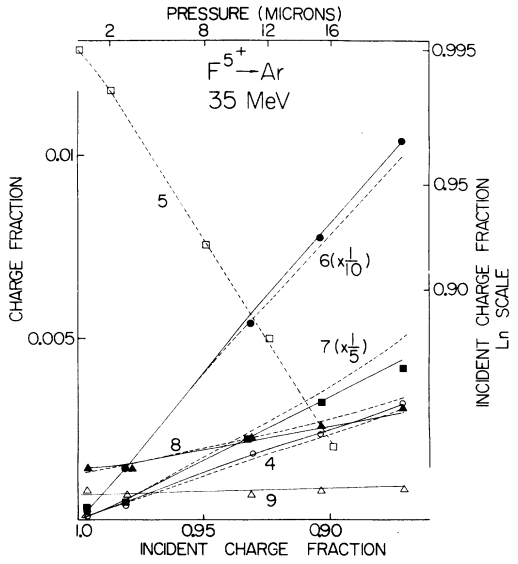

FIG. 1. Charge fractions obtained with various target thicknesses for 35-MeV fluorine ions incident in charge state +5 on argon gas. The solid lines show charge fractions calculated using the second-order charge-exchange cross sections. The dashed lines were calculated using the first-order cross section estimates. The individual data points represent the charge fractions with open circles for +4, open squares for +5, solid circles for +6, solid squares for +7, solid triangles for +8, and open triangles for +9.

is readily apparent in Fig. 1. For example, ions which change to the +6 state in one collision may leave the +6 state in a second collision and, since this possibility is ignored in Eqs. (2), the numerical integration of Eq. (1) yields values smaller than the experimental values of ϕ_6 because the first-order value of σ_{56} is underestimated. Likewise, the possibility that the +7 state can be reached from the incident +5 state by two single-loss collisions is ignored in Eqs. (2), and hence the integration of Eq. (1) yields values larger than the experimental values of ϕ_7, because σ_{57} has been overestimated. However, it is apparent that the first-order estimates of the charge-exchange cross sections used to generate the dashed lines in Fig. 1 are a reasonable starting point for the iteration procedure that is used to give a better fit to the data.

In proceeding with the iteration to obtain a complete set of cross sections that are a best fit to the data, the second-order estimate can be determined from the first-order cross sections in a number of ways. A second-order correction can be estimated from a least-squares minimization procedure[2,3] or analytically to account for multiple collisions[4]; however, the correction factors are somewhat cumbersome to calculate in real time with our limited core, and we have found this technique prone to computer errors. It would be possible to make arbitrary changes to the cross section, integrate Eq. (1) a second time, and make quantitative comparisons with the first fit prior to the next iteration. However, we have found it much more efficient in computer use to make the second-order changes more systematically than this. In the integration of Eq. (1), our computer program not only calculates the set of charge fractions, but also accumulates the multiple-collision contributions to each ϕ_i by keeping track of the separate contributions from each term of Eq. (1) at each integration step. These multiple-collision contributions are then subtracted from the experimental charge fractions at each target thickness to yield a set of ϕ's which represents a result which would be obtained if the single-collision assumption leading to Eqs. (2) were completely true. Then, in the iteration procedure of the computer program, Eqs. (3) are applied a second time to obtain a second-order set of cross sections and the integration is repeated. In addition, after each integration, the deviation of each calculated charge fraction from the experimental result at each target thickness is determined and a mean deviation[2,3,5] in the least-squares fit is obtained for each charge state of the distribution. A criterion of best fit used to terminate the calculation is that the deviation is not reduced in the next iteration. Usually this occurred after the second-order cross sections were obtained, and in the worst case four iterations were required.

In the data shown in Fig. 1 charge fractions calculated by integrating Eq. (1) with the final cross sections are shown by the solid lines. The fit to the experimental points is improved. The cross sections and the mean deviations of the observed charge states from the results calculated with the first- and second-order approximation are presented in Table I for this example. The multiple-collision contributions determined in the analysis indicate that at 16-μ Hg pressure 4% of the ions that enter the +6 state in their first collision will leave the +6 state in a subsequent collision, and 15% of the ions that reach the +7 state do so through a two-collision process. This is an extreme example since the +5 state is far from the equilibrium charge state (about +8) at 35 MeV and for most other charge states the multiple-collision effects are smaller. Because each cross section is strongly determined by only one charge-state growth curve in our data-fitting procedure, the relative error in each cross section depends on both the least-squares fitting procedure and the multiple-collision contribution influencing the relevant growth curve. This error ranges from a few percent for single transfer up to 40% for multiple transfer. Of course, the absolute uncertainty in the cross sections is obtained from the decay of the incident-charge state and hence from the uncertainty in target thickness. This uncertainty in the absolute value of the cross sections is from 10 to 20%. We point out that electron-loss cross sections have a larger uncertainty than capture cross sections because of the low-energy background from slit-edge-scat-

TABLE I. Charge-exchange cross sections evaluated for $F^{+5} \rightarrow Ar$ at 35 MeV. The first-order cross sections are the result of a fit to the data with Eq. (3). The second-order cross sections are the result of a second fit after the contributions from multiple events have been removed following the first numerical integration. The average deviation between the experimental and calculated charge fractions is given to estimate the uncertainty in the cross section making the dominant contribution to the charge-state growth.

		σ_{54}	σ_{56}	σ_{57}	σ_{58}	σ_{59}
First order	Cross section (10^{-16} cm^2/atom)	0.005	0.325	0.068	0.0054	0.0008
	Average deviation (%)	5	3.3	13	19	46
Second order	Cross section (10^{-16} cm^2/atom)	0.010	0.340	0.057	0.0040	0.0008
	Average deviation (%)	2.5	1.3	2.5	8	42

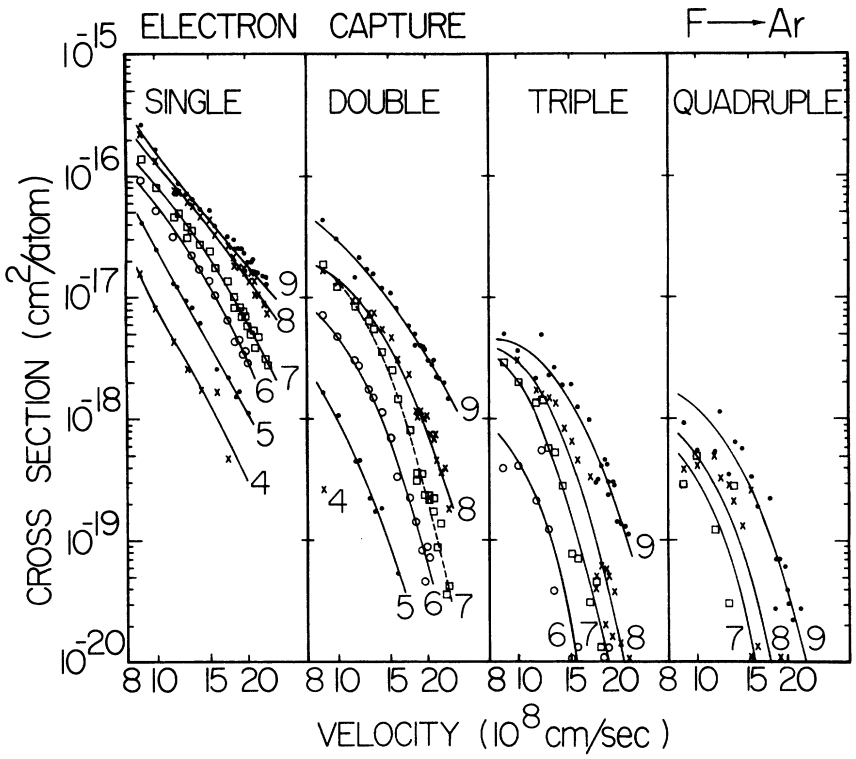

FIG. 2. Electron-capture cross sections, fluorine → argon. The lines through the data points are smooth curves to guide the eye. The separate curves are labeled with the charge state of the incident ion, and the different sections of the figure show data for different numbers of electrons captured.

tered particles observed in the position-sensitive detector at deflection angles larger than those for the incident-charge state.

IV. RESULTS AND DISCUSSION

A complete set of cross sections was determined for fluorine ions passing through argon gas at 22 energies ranging from 8 to 54 MeV. The electron-capture cross sections are shown as a function of velocity in Fig. 2, and smooth curves are drawn through the points to guide the eye. Each curve is labeled by the initial-charge state of the ion. Cross sections for single-, double-, triple-, and quadruple-electron transfer in one collision are shown in separate sections of the figure. In general, theoretical calculations[6] of capture cross sections and earlier experimental results[1-4,6] predict a rapidly decreasing function of velocity and the data of Fig. 2 confirm this. The single-capture cross sections are reasonably represented as dependent upon a negative power of the velocity with the index being ~3 for charge states 9 and 8, ~4 for charge states 7 and 6, and almost 5 for states 5 and 4. However, for the capture of two or more electrons the dependence is much steeper at high velocity than low, suggesting that a maximum in the multiple-electron capture might be reached at the low end of the velocity range of these experiments.

One would expect that the capture cross section

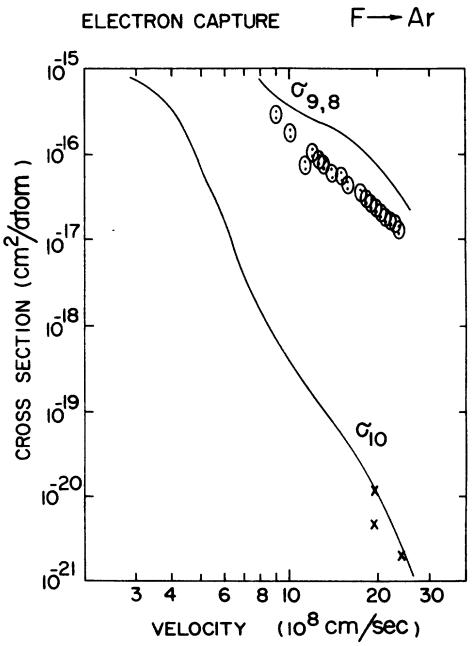

FIG. 3. Comparison of the electron-capture cross section in argon for fully stripped fluorine nuclei to a scaling of a Brinkman-Kramers calculation by Nikolaev (Ref. 6). The proton data are from Ref. 9. The lower point in the oval is the single-capture cross section and the upper point includes a sum of all capture processes.

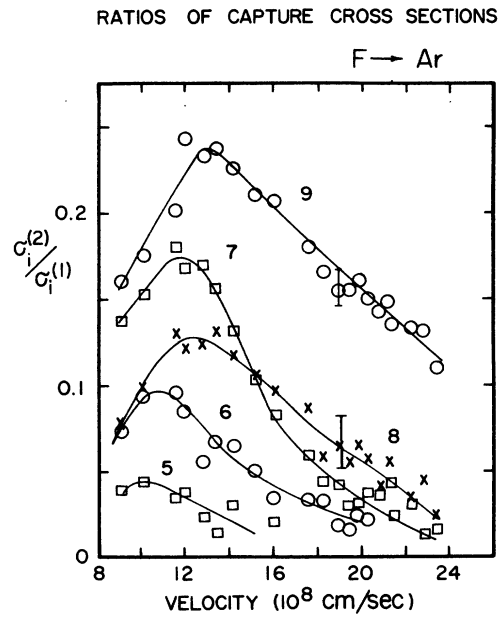

FIG. 4. Ratio of double- to single-capture cross sections for fluorine ions in argon. The separate curves are labeled with the incident-charge state.

for a fully stripped ion could be calculated by a simple scaling of the cross section for protons. Nikolaev[6,7] has taken a general form of the Brinkman-Kramers calculation derived by Schiff[8] and adapted it semiempirically to electron capture by fully stripped nuclei of charge Z to obtain the following approximate scaling equation:

$$\sigma_{Z,Z-1} = \sigma_{10} Z^2 (v/2v_0)^3 , \tag{4}$$

where $v_0 = 2.19 \times 10^8$ cm/s is the velocity in the first Bohr orbit of hydrogen and σ_{10} is the capture cross section for protons at the ion velocity v. In Fig. 3 are shown the results of this scaling from protons to fluorine ions capturing electrons from argon. The lower curve is σ_{10}, as calculated by Nikolaev for protons in argon, and the points marked with crosses are data from experiments in this laboratory reported elsewhere.[9] The upper curve was derived from the lower curve using Eq. (4) with $Z = 9$. The ovals show the cross sections for fluorine ions measured in this work. The lower point in the oval is the experimental single-capture cross section and the upper point is a sum including the multiple-capture cross sections. In the theoretical calculation the captures from different shells are treated separately and at 12×10^8 cm/s the capture from the M shell of argon falls below the capture from the L shell, producing a kink in the theoretical-cross-section curve near that velocity. The experimental points do not reflect that kink. In absolute value, the theoretical curve is too high by a factor of 2–3. Thus the agreement between experiment and theory is much poorer for fluorine ions in argon than in nitrogen,[1] for which the agreement is within 30%.

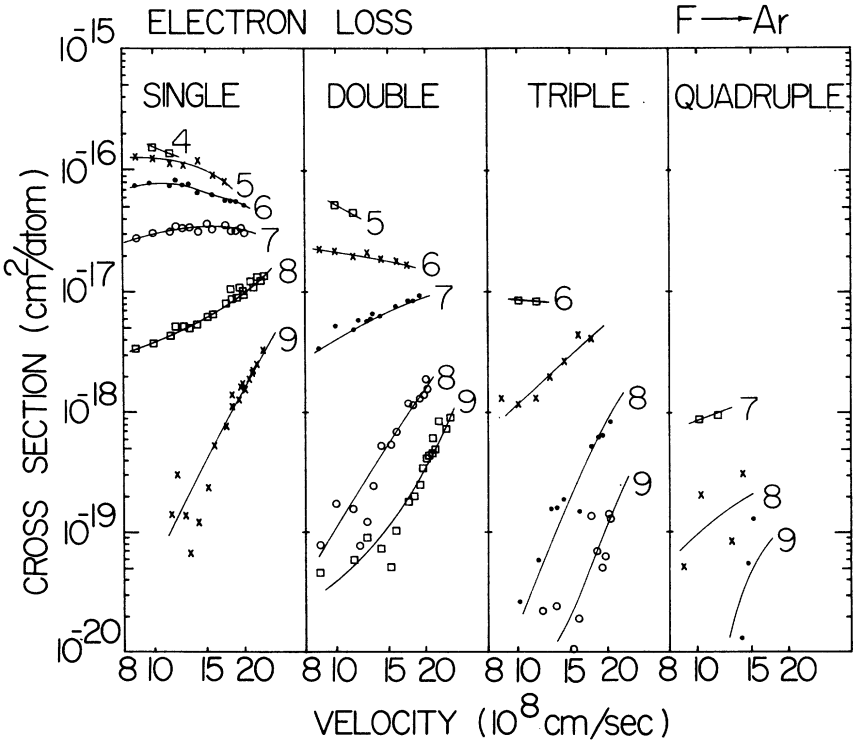

FIG. 5. Electron-loss cross sections, fluorine →argon. Each curve is labeled by the final state of the ion after electron loss, and the different sections of the figure give data for different numbers of electrons lost.

Theoretical analysis of the problem of multiple-electron capture[6,10] suggests that the ratio of double- to single-capture cross sections is a quantity independent of the geometry of the collision and related to a probability for capture in a restricted domain of impact parameter. This ratio, obtained from the experimental data, is shown in Fig. 4 with smooth curves drawn through the data points to guide the eye and with each curve labeled by the charge of the incident ion. The average deviation of the ratio of double to single cross section for four sets of measurements is shown by the error bars on two data points at 35 MeV. It is evident in Fig. 4 that the cross-section ratio rises to a maximum for all incident-charge states in the velocity region near 12×10^8 cm/s. With oxygen ions undergoing charge exchange in argon, nitrogen, and helium, Martin and Macdonald[10] have found that this maximum occurred at different velocities for the different charge states in the various targets. This was interpreted to result from the importance of capture of electrons from different binding levels of the target atom as the dominant process with the different charge states. In the data shown in Fig. 4 the dominant maximum in the ratio for charge state 7 is inconsistent with this model, and hence we conclude that the identification of the electrons transferred in the capture process is not determined uniquely by considering this ratio of double to single events.

Electron-loss cross sections for fluorine ions in argon are shown in Fig. 5. Smooth curves are drawn through the data points to guide the eye and each curve is labeled with the final charge state of the ion. Each section of Fig. 5 corresponds to the loss of different numbers of electrons leading to the final state indicated. According to the theoretical work of Bohr and Lindhard[11] maxima are expected in loss cross sections when the velocity v of the ion and the velocity of the electron about to be lost, u, are related by $v/u \approx \gamma$, where γ is slightly larger than unity. In the data shown in Fig. 5 for fluorine ions in argon, the maxima are quite broad and the loss cross sections that have maxima in the velocity range of this experiment are summarized in Table II. The values of u for each electron were estimated from tabulated binding energies[12] I by

$$u_p = (2\, I_p/m_e)^{1/2}, \tag{5}$$

where the subscript p denotes the particular electron lost. Values of γ from 1 to 2 are obtained in the four cases for which maxima were evident.

It is well known[2] that multiple-electron loss occurs in single collisions with cross sections that often approach in magnitude the single-loss cross section, especially for ionic charge states lower than the equilibrium mean charge. Based on evidence from experiments with oxygen ions, Macdonald and Martin[4] argue that loss cross sections leading to the same final state should be qualitatively similar in velocity dependence. The argument for this similarity assumes that the loss of each electron during a collision is a relatively

TABLE II. Maxima observed in electron-loss cross sections in argon for fluorine ions from 8 to 54 MeV. The designation of the last electron removed implies an ordering by binding energy of the L-shell electrons of the final state.

Last electron removed	Loss cross section	Range of ion velocity near maximum (v)	Orbital velocity (u)	$\gamma = v/u$
L-1	σ_{67}	$6v_0 - 8v_0$	$3.8v_0$	1.6–2.1
L-2	σ_{56}	$4v_0 - 6v_0$	$3.4v_0$	1.2–1.8
L-3	σ_{45}	$3v_0 - 4v_0$	$2.8v_0$	1.0–1.4
L-2	σ_{46}	$3v_0 - 4v_0$	$3.4v_0$	0.8–1.2

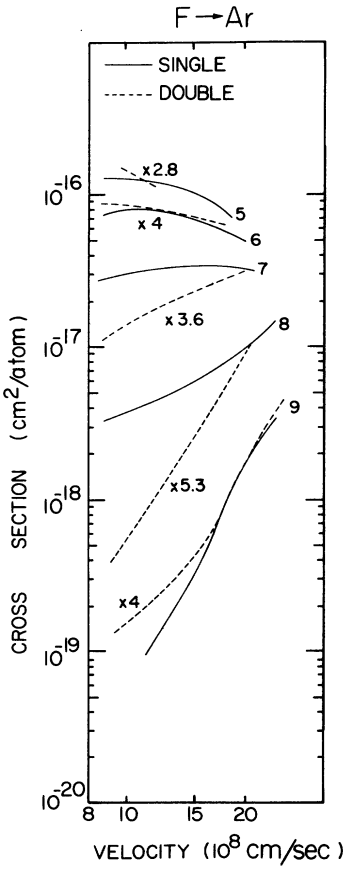

FIG. 6. Comparison of single- and double-loss cross sections leading to the same final state indicated on the figure. The double-loss cross sections multiplied by the factors indicated are shown by the dashed curves and the single-loss cross sections are shown by the solid curves.

independent event, and the multiple cross sections will be dominated in velocity dependence by the last electron lost. The velocity dependence of the single- and double-loss cross sections leading to the same final charge state of fluorine ions in argon are compared in Fig. 6, in which the cross sections for single loss are indicated by solid lines and for double loss by broken lines. In order to overlay the single- and double-loss cross sections for each charge state for comparison, the double-loss cross sections have been multiplied by the factor indicated in the figure. It is evident that the single- and double-loss cross sections leading to the +6 and +9 charge states have a similar velocity dependence; however, the cross sections leading to charge states +7 and +8 are quite different. For the electron loss reported previously for fluorine ions in nitrogen,[1] dissimilar velocity dependences were also observed for some charge states, and hence we conclude that no general similarity of the velocity dependence of single- and multiple-electron-loss cross sections can be expected.

---

*Work partially supported by the U. S. Atomic Energy Commission under Contract No. AT(11-1)-2130.

†Present address: Department of Nuclear Physics, Australian National University, Canberra, Australia.

[1]J. R. Macdonald, S. M. Ferguson, T. Chiao, L. D. Ellsworth, and S. A. Savoy, Phys. Rev. A 5, 1188 (1972).

[2]H. D. Betz, Rev. Mod. Phys. 44, 465 (1972).

[3]S. Datz, H. O. Lutz, L. B. Bridwell, C. D. Moak, H. D. Betz, and L. D. Ellsworth, Phys. Rev. A 1, 430 (1970).

[4]J. R. Macdonald and F. W. Martin, Phys. Rev. A 4, 1965 (1971).

[5]R. H. Bacon, Am. J. Phys. 21, 428 (1953).

[6]V. S. Nikolaev, Usp. Fiz. Nauk 85, 679 (1965) [Sov. Phys. Phys.—Usp. 8, 269 (1965)].

[7]V. S. Nikolaev, Zh. Eksp. Theor. Fiz. 51, 1263 (1966) [Sov. Phys.—JETP 24, 847 (1967)].

[8]H. Schiff, Can. J. Phys. 32, 393 (1954).

[9]J. R. Macdonald, S. M. Ferguson, L. D. Ellsworth, T. Chiao, S. A. Savoy, and W. W. Eidson, in *Proceedings of the Seventh International Conference on the Physics of Electronic and Atomic Collisions*, Amsterdam, 1971, edited by L. M. Branscomb *et al.* (North-Holland, Amsterdam, 1972), p. 516.

[10]F. W. Martin and J. R. Macdonald, Phys. Rev. A 4, 1974 (1971).

[11]N. Bohr and J. Lindhard, Kgl. Danske Videnskab. Selskab. Mat. Fys. Medd. 28, No. 7 (1954).

[12]W. L. Wiese, M. W. Smith, and B. M. Glennon, *Atomic Transition Probabilities*, U.S. Natl. Bur. Std. National Standard Reference Data Series—4 (U.S. GPO, Washington, D.C., 1966), Vol. 1, p. 113.